Enhancement of structural and electrical properties of ZnO/ PVA nanocomposites

A.F. Mansour, S.F. mansour and M.A. Abdo
Physics Department, Faculty of Science, Zagazig University, Egypt

Abstract: *ZnO nanoparticles were prepared by the sol- gel methode, and nanocomposite films of ZnO doped with polyvinyl alcohol were prepared using the solution casting methode. Different nanocomposites films were prepared according to the formula with compositions (w/w between ZnO and PVA solution concentration: 0%, 0.15%, 0.5%, 1%, 2%, 2.5%, and 3%), and characterized by X-ray diffraction (XRD), and high resolution transmission electron microscopy (HRTEM). The electrical properties of nanocomposites as a function of filler as well as the matrix were determined. In ZnO/ PVA nanocomposites, ZnO is a semiconducting material; the electrical conductivity and dielectric constant of PVA matrix were enhanced by adding ZnO nanoparticles due to its free electrons. The nanocomposite ZnO/ PVA (3% wt) shows higher conductivity as compared to other concentration of ZnO.*

Keywords: *Polyvinyl Alcohol (PVA); Zinc Oxide ZnO; nanocomposites; XRD; electrical properties.*

I.   Introduction

Composite materials are engineered materials made from two or more constituent materials with significantly different physical or chemical properties which remain separate and distinct on a macroscopic level within the finished structure [1]. Composites have good potential for various industrial fields because of their excellent properties such as high hardness, high melting point, low density, low coefficient of thermal expansion, high thermal conductivity [2]. Polymer- based nanocomposite have many applications of because of their electron transport, mechanical and optical properties in medical and engineering technology [3, 4].

Polyvinyl alcohol (PVA) is a polymer with several interesting physical properties, which are very useful in technical application. PVA is a semi crystalline, water soluble and low electrical conductivity material with many technological, pharmaceutical and biomedical applications [5,6].

Zinc oxide (ZnO) is one of the II–VI group binary semiconductors having a direct and wide band gap. The band gap of ZnO is 3.44 eV at low temperatures and 3.37 eV at room temperature [7]. This enables applications in optoelectronics in the blue/UV region, including light-emitting diodes, laser diodes and photo detectors [8- 10]. ZnO has a large exciton binding energy. The free- exciton binding energy in ZnO is 60 meV [11, 12]. This large exciton binding energy indicates that efficient excitonic emission in ZnO can manifest at room temperature and higher. Under ordinary conditions, ZnO is composed of hexagonal wurtzite crystal structure, the space symmetry group is (P63mc), with unit cell a= 3.253 Å and c= 5.215 Å [13]. So, ZnO can be used short-wavelength light emitting diodes, transparent conductors, dye-sensitized solar cells, piezoelectric materials, gas sensors, photovoltaic cells, varistors (also called as variable resistors), as a high resistance semiconducting device and fully transparent thin film transistors [14].

Few researchers have studied the electrical properties of PVA and ZnO nanocomposites [15, 16]. Therefore, in the present study; the structural, electrical and optical properties have a significant improvement in these properties.

In the present work ZnO nanoparticles have been synthesized by sol–gel method. ZnO/ PVA nanocomposite films with different concentrations of nano ZnO were prepared using easy and low cost solution casting method. The samples were characterized by XRD, HRTEM and UV– visible spectroscopy. Also, we had studied the electrical properties of ZnO/ PVA nanocomposites based on ZnO nanoparticles as inorganic filler material and PVA as the main matrix.

II.   Experimental

2.1. Materials

Polyvinyl alcohol (PVA) from Sigma Aldrich, with average molecular weight of 50.000 – 85.000 and 97% hydrolyzed was used without further purification. Zinc nitrate [$Zn(NO_3)_2.6H_2O$] and ethylene glycol ($C_2H_6O_2$) also were purchased from Aldrich. Reactant solutions were made in doubly distilled water.

2.2. Synthesis of ZnO nanoparticles

Nano-sized particles of ZnO were prepared using sol gel method [17, 18]. The proper amounts of zinc nitrate hexahydrate ($Zn(NO_3)_2 \cdot 6H_2O$) was dissolved in distilled water under constant stirring and heated to about

90°C for 1 h. The solution was added to ethylene glycol ($C_2H_6O_2$) maintaining the molar ratio between the metal nitrates and the ethylene glycol as 1:1. This mixed solution was then stirred for 2h to achieve good homogeneity. The precursor mixture was heated to allow evaporation then combustion to obtain finally the desired product zinc oxide (ZnO) in the form of ash powder.

2.3. Preparation of ZnO/ PVA nanocomposite films

The nanocomposite films were prepared by the well known solution casting technique. In this method 7g of (PVA) powder was dissolved in 80 ml of de-ionized water by stirring and heated kindly using a magnetic stirrer with hot plate, for complete dissolution without thermal decomposition of the polymer, until the polymer was completely dissolved and a clear viscous solution is formed. The prepared ZnO nanopowder was added into the aqueous solution of PVA in the following composition (w/w between ZnO and PVA solution concentration): 0%, 0.15%, 0.5%, 1%, 2%, 2.5%, and 3% then stirred carefully by using magnetic stirrer until transparent ZnO/ PVA dispersion was obtained. Each mixture is put in a Petri dish and leave to dry in a dust free chamber at room temperature for 48h to obtain the nanocomposite films.

2. 4. Characterization

The X-ray diffraction (XRD) patterns of the pure PVA film, nano ZnO powder and the polymer nanocomposite films were recorded at room temperature using an X-ray powder diffractometer (Shimadzu XRD 6000) equipped with Cu K_{α} as radiation source (λ = 1.54Å.) in the 2θ (Bragg angles) range($10^{\square} \leq 2\theta \leq 80^{\square}$) to report the information about their structure. The morphology and particle size distribution of the samples were identified using high resolution transmission electron microscope (HRTEM) JEOL-2100 at 200 KV. The absorbance spectra (A) and the transmittance spectra (T) of the films were recorded at 200–1100 nm wavelength using a dual beam (UVS-2800) UV–Visible spectrophotometer. The dielectric measurements were carried out using Hioki 3532 Hi-Tester in the frequency range of 60 Hz–5MHz and at various temperatures between 303 and 453 K.

III.   Results and Discussion

3.1. X-Ray diffraction analysis

The X-ray diffraction pattern (XRD) for pure polyvinyl alcohol (PVA) sample is shown in figure (1a). The XRD pattern showed a strong broad diffraction peak located at 2θ= 20.12° which corresponding to (101) reflection plane of PVA and a more peak at 41.62° indicating the semi-crystalline nature of PVA i.e., presence of crystalline and amorphous regions [16, 19]. This diffraction peak confirmed that, obtained polyvinyl alcohol (PVA) is pure polyvinyl alcohol (PVA) without any other impurities.

The XRD pattern for pure Zinc oxide (ZnO) sample is shown in figure (1b). These observable peaks, at scattering angles 2θ= 31.68°, $34.34.4^{\circ}$, 36.16°, 47.52°, 56.48°, 62.88°, 66.24°, 67.84°, 68.96°, 72.48° and 76.8° are correspond to reflections from: 100, 002, 101, 102, 110, 103, 200, 112, 201, 004 and 202 crystal planes, confirmed the formation of the as prepared ZnO in a pure single hexagonal phase. The XRD pattern was indexed and compared with JCPDS card no. 36-1451 which correspond to the hexagonal wurtzite structure of ZnO. The expanded peaks in XRD pattern indicate ultra-fine nature of the crystallites. It is clear; the peaks are very sharp, indicating the complete formation of crystal structure.

The X-ray diffraction patterns for ZnO/ PVA nanocomposite films as shown in figure (1c). XRD patterns of all ZnO/ PVA nanocomposite films showed a broad peak at 2θ ≈ 19.90°, which is attributed to the polyvinyl alcohol (PVA). Also, a small diffraction peaks observed at 2θ ≈ 31.96°, 34.67°, 36.44°, 48°, 56.86°, 63.12°, and 68.2° which is attributed to the reflection from: 100, 002, 101, 102, 110, 103, and 112 confirmed the presence of the zinc oxide (ZnO) nano particles. The diffraction peaks which attributed to ZnO is very small compared with that of PVA, because the concentration of ZnO is very low compared with that of PVA. This small peak increases by increasing ZnO content reaching 3%, as shown in figure (1c). The results indicate that the nanocomposite films consists only of two phases namely PVA and ZnO and no other phases was detected which assure its successful preparation. The lattice parameters "a" and "c" of the polycrystalline ZnO in the ZnO/ PVA nanocomposites films are calculated respectively with (100) and (002) orientations using the relation [20]:

$$\frac{1}{d^2} = \frac{4}{3}(\frac{h^2 + hk + k^2}{a^2}) + \frac{l^2}{c}$$

The obtained lattice parameters values for pure ZnO powders are a= 0.325 nm and c= 0.521 nm are in a very good agreement with those reported in JCPDS card no. 36-1451. By increasing ZnO content, the obtained the lattice parameters of the polycrystalline ZnO in the ZnO/ PVA nanocomposites films are calculated. There was a slight change in the position of the peaks indicating a corresponding change in lattice constants of the two phases. By increasing ZnO content, the obtained lattice parameters nearly have the same values (a= 0.322 nm ±

0.001) and (c= 0.516 nm ± 0.001). This indicates that ZnO nanoparticles have retained its structure even though it is capped PVA after formation of nanocomposite films, i.e., there is no interaction between polyvinyl alcohol and zinc oxide in forming nanocomposites. The crystal size of ZnO in pure nanopowder and nanocomposite films is calculated using the, Debye-Scherrer formula [21]:

$$D = \frac{0.9\lambda}{\beta \cos\theta}$$

D is the grain size, λ is the wavelength of the X-ray radiation used, β is the full width at half maximum (FWHM) of the diffraction peak and θ is the Bragg dif-fraction angle of the XRD peak. The average crystallite size estimated is ≈ 41nm.

3.2. Electron microscopy and EDX analysis

Figure (2a) shows the high resolution transmission electron microscope (HRTEM) micrograph of the as prepared ZnO. It indicates that the particles did not take perfect hexahedron shapes, but actually the deformed flaky ones. The particle size is about 20nm. The size obtained from HRTEM was less than that of XRD value (41nm), which is due to the fact that the TEM image represents the average size of primary particles whereas XRD values depend on the particle volume [22].

Figure (2b) shows the selected area electron diffraction (SAED) of the as prepared ZnO. SAED pattern is also used to identify suggest the highly crystallite nature of the ZnO nanoparticles. The rings in the electron diffraction pattern are indexed with their respective Miller planes (hkl) from the PDF database.

Energy dispersive X-ray spectrometry (EDX) investigation has been introduced to confirm the atomic composition concentration. Figure (2c) shows the EDX spectrum of the as-prepared ZnO nanoparticles is depicted where clear peaks of Zinc and Oxygen are only observed. The atomic percentages of Zn and O as obtained from EDX pattern are 61.98 and 38.02 respectively; indicating our prepared sample is only pure ZnO nanoparticles.

3.4. Dielectric properties:

Figure (3) shows the temperature dependence of dielectric constant έ, for pure PVA, ZnO, and ZnO/ PVA nanocomposites with compositions (w/w between ZnO and PVA solution concentration: 0.15% and 3%), in the frequency range 1 kHz- 5 MHz, where all samples are said to be in sequential order denotes, they possess the same behavior. Firstly, it is observed that the dielectric constant έ, decrease with increasing frequency, i.e., έ, have higher values in low frequency range then decrease with increasing frequency. This situation has been attributed to the fact that there are all types of polarizations; electronic, ionic, dipolar, and space charge polarization (Maxwell–Wagner polarization) in the low frequency range [23]. After that the situation in the high frequency range due to the fact that the electric dipoles cannot follow up the frequency of the applied electric field and so, it stops. Secondly, It is observed that the dielectric constant increase gradually with increasing temperature. The small and nearly constant values of έ with varying temperature and frequency means the electronic polarization is the most predominant one in this region of temperature. Further increase in temperature gives an increase in έ, which lead to an appreciable frequency dependence, which is because the thermal energy, given to the sample, liberates more frozen dipoles and the accompanied electric field align them in its direction causing the higher values of έ [23].

The temperature dependence of dielectric loss tangent tanδ, for pure PVA, ZnO, and ZnO/ PVA nanocomposites with compositions (w/w between ZnO and PVA solution concentration: 0.15% and 3%), in the frequency range 1 kHz- 5 MHz is shown in figure (4). Firstly, it is observed that the dielectric loss tangent tanδ, decrease with increasing frequency. This situation has been attributed to the fact that at low frequency range there are all types of polarizations consequently, loss due to those types of polarization increase. While, at high frequency range types of polarization are decreased and its accompanied loss decrease also. Secondly, it is observed that, we have the two types of the dielectric losses. The first type is due to the conduction losses which show a smooth variation with temperature (as shown in pure PVA and ZnO/ PVA nanocomposites and pure ZnO). The second type is due to the relaxation effects (dipole losses) which show a peak at a certain temperature [24], as shown in pure PVA and ZnO/ PVA nanocomposites. The dielectric loss caused by the dipole mechanism reach a maximum at a certain definite temperature and then decreases. In fact, the rise in temperature and the resulting drop in viscosity of the material exert a double effect on the amount of losses due to the friction of the rotating dipoles: on the one hand, the degree of dipole orientation increases (consequently, dipole losses increases), and on the other hand, the viscosity of the material decreases (consequently, dipole losses decreases). Also, it is observed that, loss tangent tanδ, have small values at low temperature and increases with the increase in temperature.

Figure (5) show the relation between Lnσ$_{ac}$ (σ$_{ac}$ is the alternating current conductivity) and the reciprocal of absolute temperature for pure PVA, ZnO, and ZnO/ PVA nanocomposites with compositions (w/w

between ZnO and PVA solution concentration: 0.15% and 3%), in the frequency range 1 kHz- 5 MHz. The data at each separate frequency obeys the well known Arrhenius equation: $\sigma_{ac} = \sigma_o \exp(-E/kT)$, where E is the activation energy, k is the Boltzmann´s constant and T is the absolute temperature. The data show that, the ac conductivity (σ_{ac}) increases with increasing frequency; which acts as a pumping force, pushing the charge carriers between the different conduction states. Also, it is observed that, the conductivity increases with increasing temperature with changing the slope at a certain temperature which is general trend of semiconductor like behavior. The activation energies were calculated and tabulated in table (1). The activation energies values show that all the samples have two regions with changing slope at different temperatures, i.e., the conduction mechanism changes from one region to another region [25]. The first region (I) in the conductivity plot at low temperature (< 378 K for PVA/ZnO nanocomposites) and (< 588 K for pure ZnO) indicates the conduction is may be due to one of the following two donor ionization processes: $Zn_i^+ \rightarrow Zn_i^{2+} + e^-$ proposed by Sukker and Tuller [26] for zinc interstitial (Zn_i) or, $V_O \rightarrow V_O^+ + e^-$ proposed by Simpson and Cordero[27] for oxygen vacancy (V_O) which forms a donor level below the conduction band. While the second region (II) at relatively higher temperature (> 378 K for PVA/ZnO nanocomposites) and (> 588 K for pure ZnO) the conduction can be associated with desorption of O_2^- species [28] according to the equation, $O_2^- \rightarrow O_2 + e^-$. The obtained activation energy for pure ZnO nanoparticles is in a very good agreement with literature [29].

The dependence of dielectric constant $\acute{\epsilon}$, for ZnO/ PVA nanocomposites at 1 kHz and room temperature on ZnO concentration is shown in figure (6). It is noticed that, the dielectric constant of the PVA matrix is enhanced by the adding ZnO nanoparticles and the concentration (3% wt) ZnO has the highest one. This effect is may be due to, the free electron of ZnO which contributes to the electronic polarizations of the nanocomposites. Also, ZnO containing large amount of oxygen vacancies; which acts as shallow donors [30]. These oxygen vacancies have positive charges with the negative oxygen ions produce a large amount of dipole moments; leading to rotational dipole moment in the presence of an external field. Also, space charge polarizations of ZnO/ PVA nanocomposites increase by adding the foreign ZnO nanoparticles into the PVA matrix.

The dependence of dielectric loss tangent tanδ, for ZnO/ PVA nanocomposites at 1 kHz and room temperature on ZnO content is shown in figure (7). It is noticed that the ZnO concentration (1 % wt) has the lowest loss among the ZnO/ PVA nanocomposites.

The dependence of ac conductivity for ZnO/ PVA nanocomposites at 1 kHz and room temperature on ZnO concentration is shown in figure (8). It is noticed that the conductivity of PVA matrix enhanced with ZnO nanoparticles, by its free electrons, and the concentration ZnO (3% wt) has the highest one.

IV.   Conclusion:

Nano-sized particles of ZnO were prepared using sol gel method. The nanocomposite films were prepared by the well known solution casting technique. The average crystallite size estimated from XRD is ≈ 41nm but the particle size from HRTEM is about 20nm. ZnO nanoparticles enhanced the electrical properties of the virgin PVA matrix. The nanocomposite with concentration (3% wt) is the characteristic one, where have the highest dielectric constant, lowest dielectric loss, and highest electrical conductivity. These entire advantage make the ZnO/ PVA nanocomposite with ZnO concentration (3% wt) have wide range for solar cell applications, especially for solar cells electrode instead of indium tin oxide (ITO).

References:
[1]. C. Barry Carter, M. Grant Norton, Ceramic Materials Science and Engineering, (2007).
[2]. Ahmed Hashim, Majeed Ali, Bahaa H. Rabee, American Journal of Scientific Research, 69 (2012), 5-9.
[3]. N. Bouropoulos, G.C. Psarras, N. Moustakas, A. Chrissanthopoulos, S. Baskoutas, Phys Status Solidi A 205 (2008) 2033–2037.
[4]. J. Lee, D. Bhattacharyya, A.J. Easteal, J.B. Metson, Curr Appl Phys 8 (2008) 42–47.
[5]. C. M. Hassan, N.A. Peppas, Adv. Polym. Sci. 153 (2000) 37- 65.
[6]. M. Kokabi, M. Sirousazar, Z. Hassan, Eur. Polym. J. 43 (2007) 773- 781.
[7]. A. Mang, K. Reimann and Rubenacke St, Solid State Commun, 94(1995) 251- 254.
[8]. Ü. Özgür, Ya. I. Alivov, C. Liu, A. Teke, M. A. Reshchikov, S. Dogan, V. Avrutin, S-J. Cho and H. Morkoç, J. Appl. Phys., 98 (2005) 041301.
[9]. N. H. Nickel and E. Terukov, Zinc Oxide - A Material for Micro- and Optoelectronic Applications, (ed) 2005, (Netherlands: Springer).
[10]. C. Jagadish and S. J. Pearton, Zinc Oxide Bulk, Thin Films, and Nanostructures, (ed) 2006, (New York: Elsevier).
[11]. D. C. Reynolds, D. C. Look and B. Jogai, Solid State Commun, 99 (1996) 873- 875.
[12]. D. M. Bagnall, Y. F. Chen, Z. Zhu, T. Yao, S. Koyama, M. Y. Shen and T. Goto, Appl. Phys. Lett., 70 (1997) 2230- 2232.
[13]. Muhammad Saleem, Liang Fang, Aneela Wakeel, M. Rashad, C. Y. Kong, World Journal of Condensed Matter Physics, (2012), 2, 10-15.
[14]. Husam S. Al-Salman, M.J. Abdullah, Superlattices and Microstructures 60 (2013) 349–357.
[15]. Aashis S. Roy, Satyajit Gupta, S. Sidhu, Ameena Parveen, Praveen C. Ramamurthy, Composites: part B 47 (2013) 314-319.
[16]. K.S. Hemalatha, K. Rukmani, N. Suriyamurthy, B.M. Nagabhushana, Materials Research Bulletin 51 (2014) 438–446.
[17]. Agnieszka Kołodziejczak-Radzimska and Teofil Jesionowski, Materials 7 (2014) 2833-2881.
[18]. Mamady Nassou Conde, Khalid Dakhsi, Hafid Zouihri, Karima Abdelouahdi, Larbi Laanab, Mohammed Benaissa1 and Boujemaâ Jaber, Journal of Materials Science and Engineering A 1 (2011) 985-990.

[19]. Pal Kunal, Banthia Ajit K., and Majumdar Dipak K., AAPS Pharm SciTech 8 (1) (2007), Article 21.
[20]. y. Waseda, K. Shinoda, E. Matsubara, X-Ray Diffraction Crystallography: Introduction, Examples and Solved Problems, (Springer, New York, 2011).
[21]. B.D. Cullity, Elements of X-ray Diffraction, Reading, MA, 1978.
[22]. S. Ayyappan, Philip John, Raj Baldev, Materials Chemistry and Physics, 115 (2009) 712–717.
[23]. M. A. Ahmed, Samiha. T. Bishay, G. Abdelatif, Journal of Physics and Chemistry of solids, 62 (2001) 1039- 1046.
[24]. B. Tareev, Physics of Dielectric Materials, Mir publishers, Mosco, (1973).
[25]. T. Sujatha, G.B. Devidas, T. Sankarappa, S.M. Hanagodimath, International Journal of Engineering Sciences, 2(7) (2013) 302-309.
[26]. Sukker M.H., Tuller H.L., Adv. Ceram. 7 (1984) 49.
[27]. J.C. Simpson, J.F. Cordero, J. Appl. Phys. 63 (1988) 1781.
[28]. S. Fujitsu, K. Koumoto, H. Yanagida, Y. Watanabe, H. Kawazoe, J. Appl. Phys. 38 (1999) 1534- 1538.
[29]. M.L. Dinesha, H.S. Jayanna, S. Ashoka, G.T. Chandrappa, Journal of Alloys and Compounds, 485 (2009) 538–541.
[30]. Amrut S. Lanje, Satish J. Sharma, Raghumani S. Ningthoujam, J.-S. Ahn, Ramchandra B. Pode, Advanced Powder Technology, 24 (2013) 331–335.
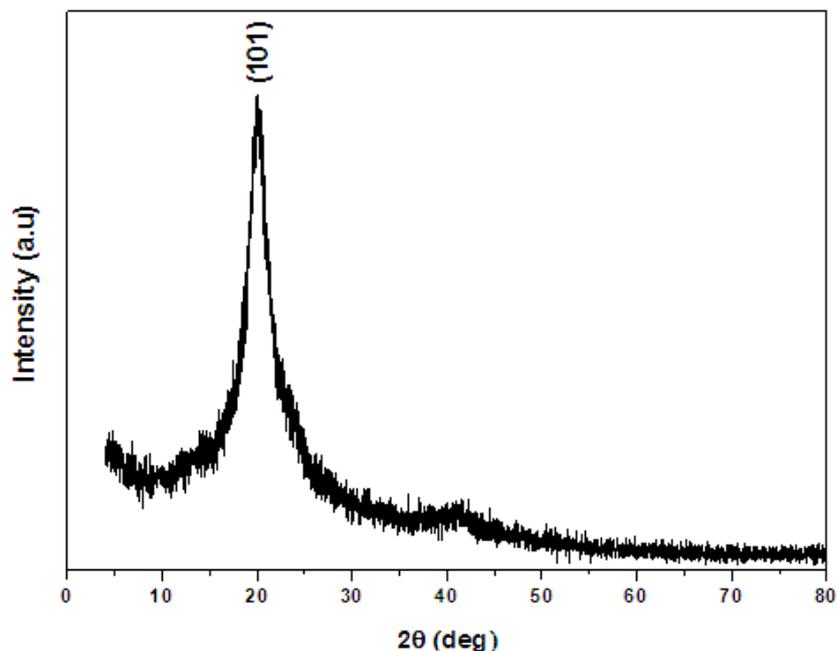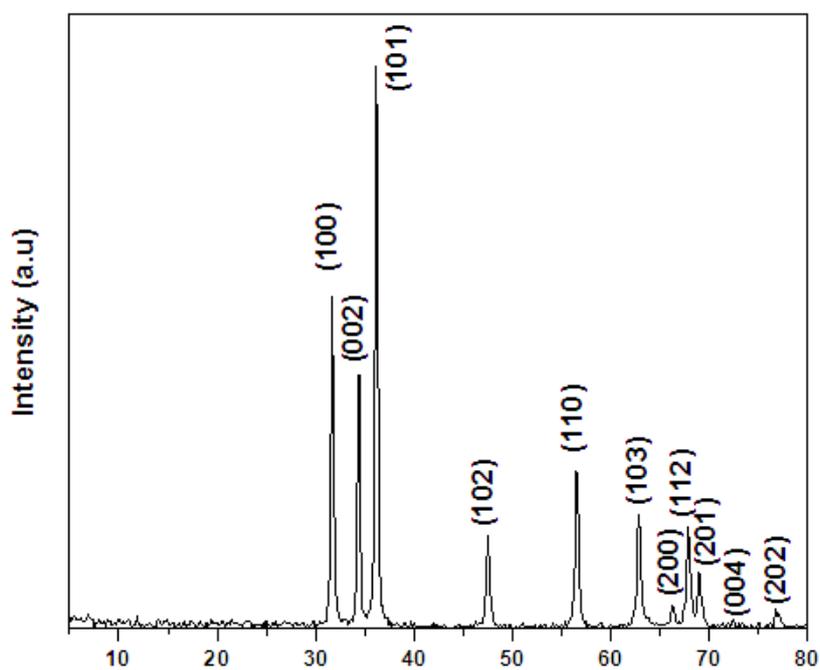
Fig. (1a): XRD pattern of pure PVA.

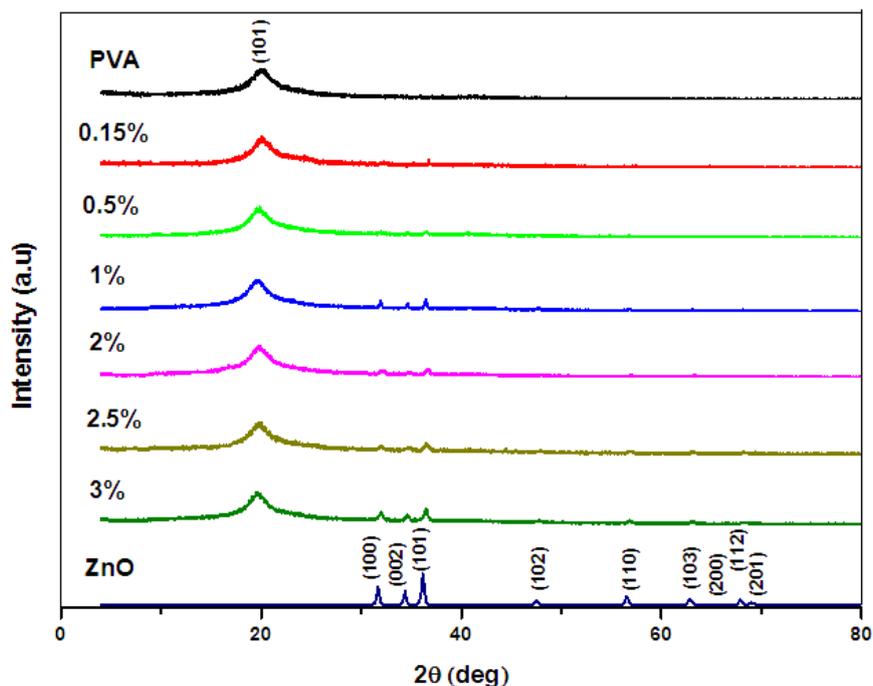
Fig. (1b): XRD pattern of pure ZnO.

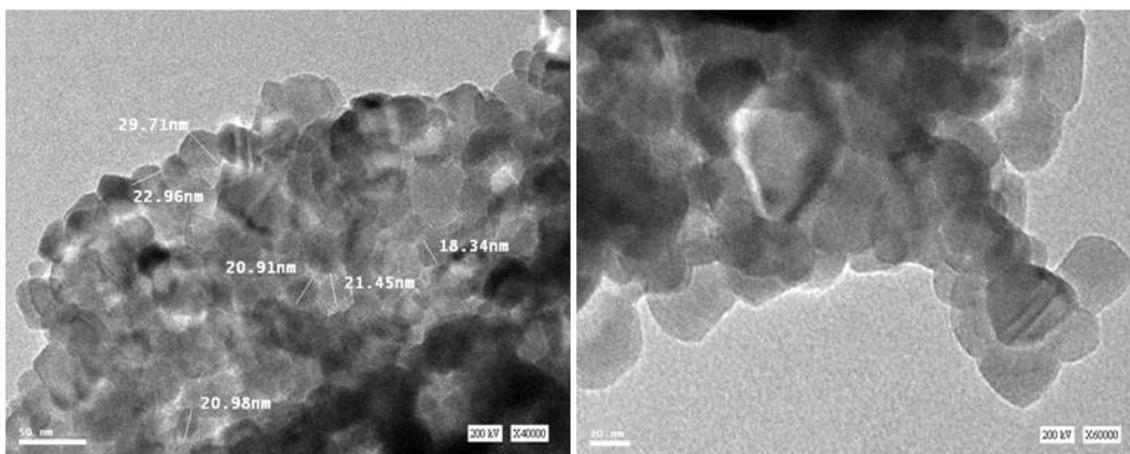**Fig. (1c):** XRD pattern of: PVA ZnO/ PVA films, and ZnO, respectively.

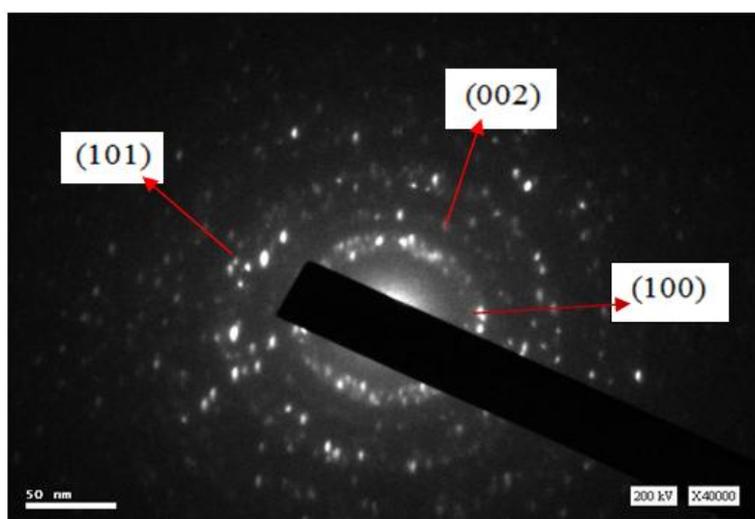**Fig. (2a):** HRTEM micrograph of the as-prepared ZnO.

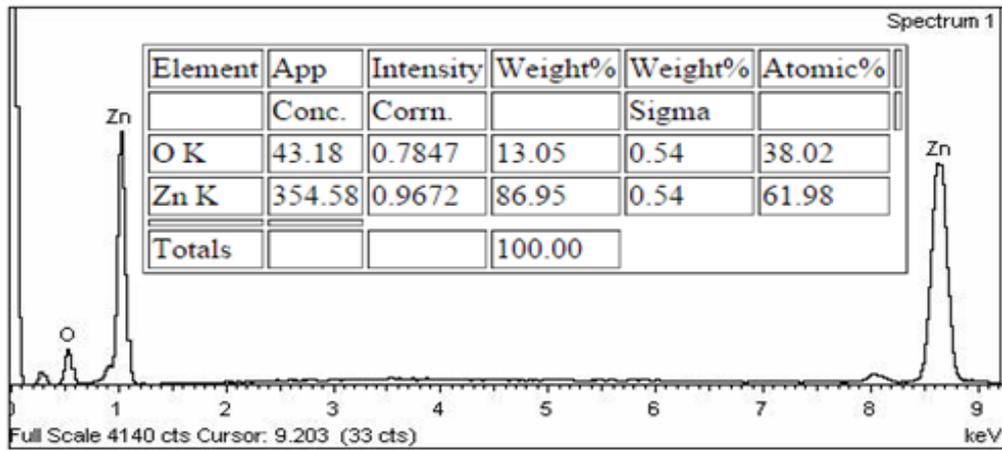**Fig. (2b):** SAED pattern of the as-prepared ZnO.
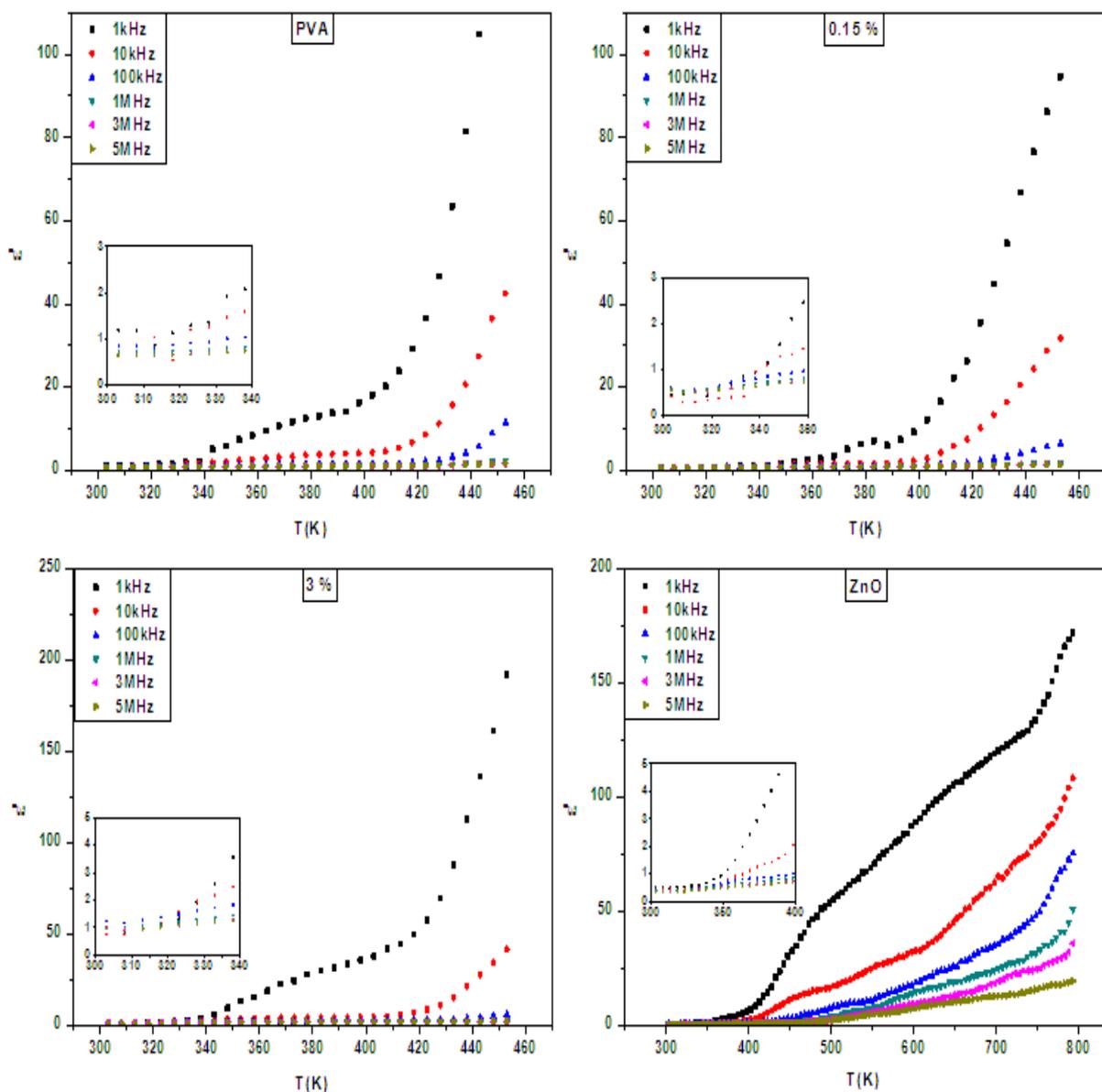
Fig. (2c): EDX spectrum of the as-prepared ZnO

Fig. (3): Dependence of dielectric constant έ, on absolute temperature for pure PVA, ZnO/ PVA nanocomposites (0.15 and 3% wt) and pure ZnO in the frequency range 1 kHz- 5 MHz.

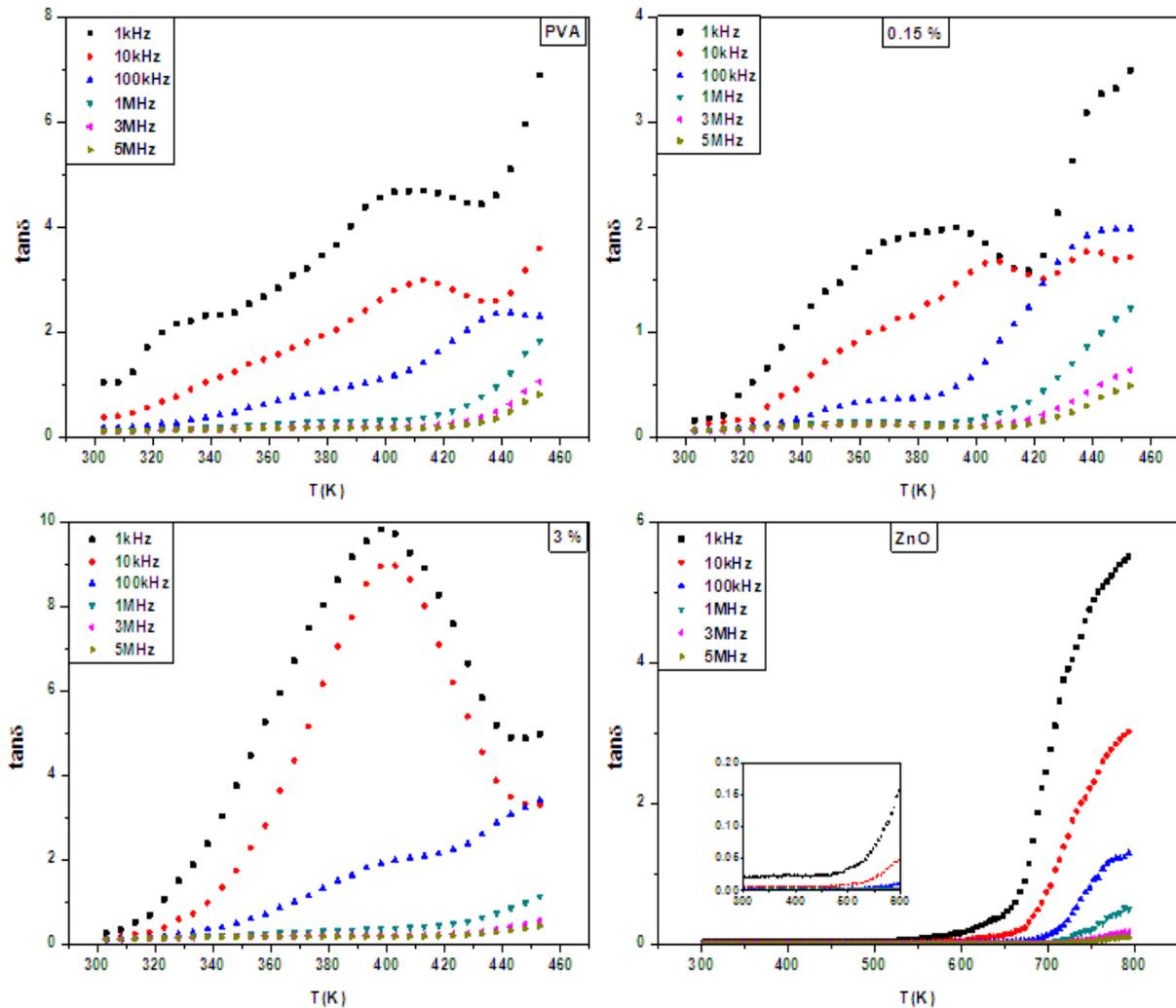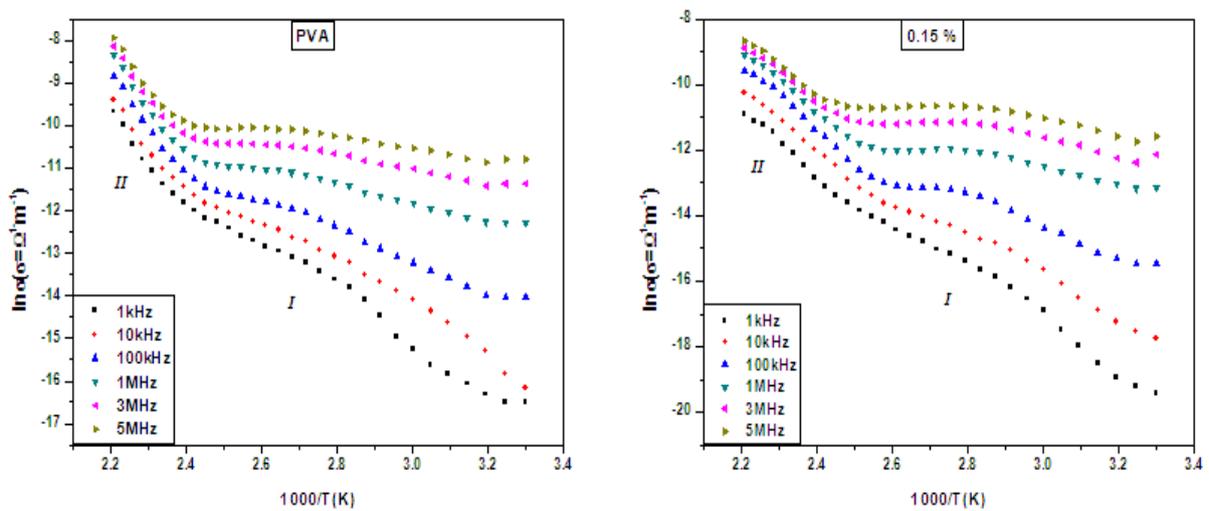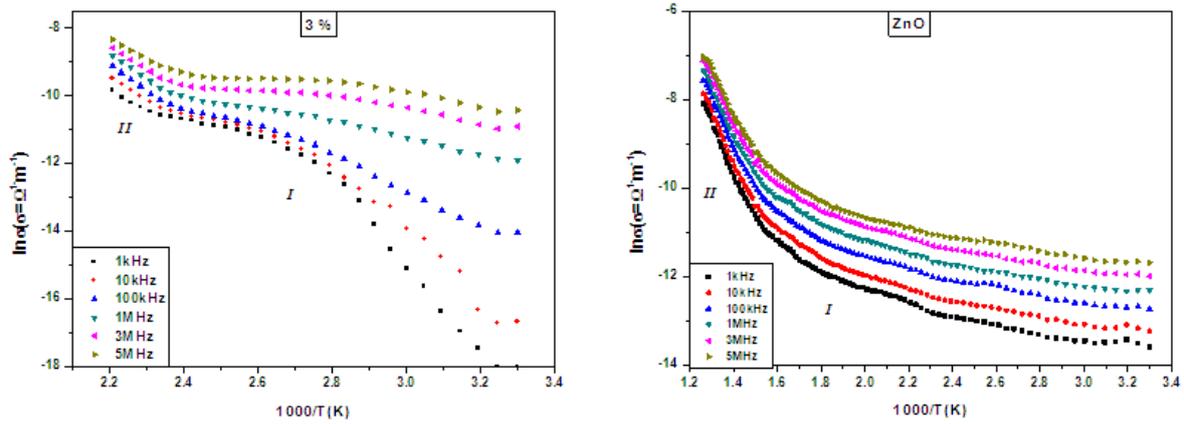**Fig. (4):** Dependence of dielectric loss tangent tanδ, on absolute temperature for pure PVA, ZnO/ PVA nanocomposites (0.15 and 3% wt) and pure ZnO in the frequency range 1 kHz- 5 MHz.
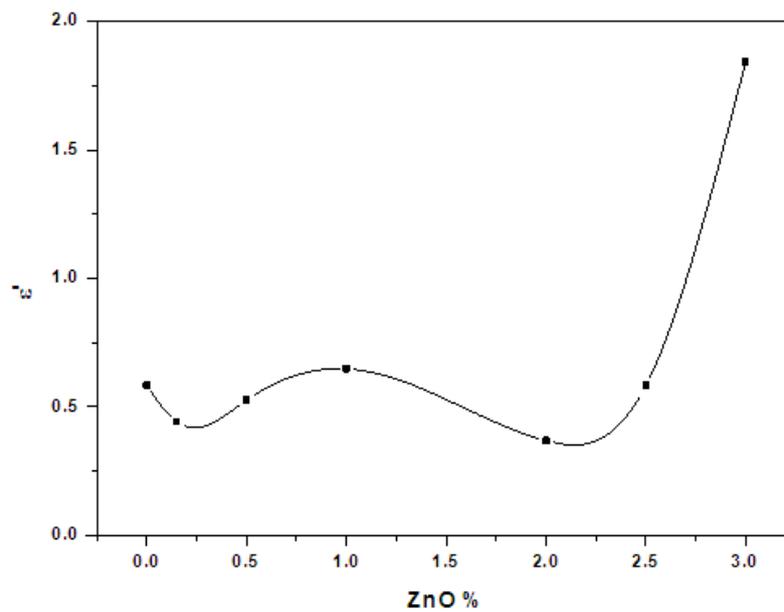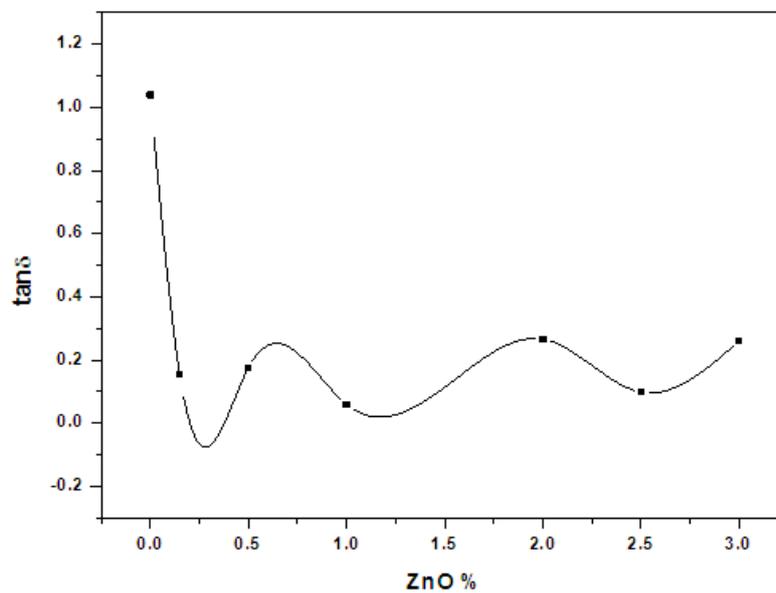
Fig. (5): Dependence of ac conductivity on the reciprocal of the absolute temperature for pure PVA, ZnO/ PVA nanocomposites (0.15 and 3% wt) and pure ZnO in the frequency range 1 kHz- 5 MHz.

Fig. (6): The obtained values of dielectric constant as a function of ZnO concentrations at 1 kHz and room temperature.

Fig. (7): The obtained values of dielectric loss tangent as a function of ZnO concentrations at 1 kHz and room temperature.
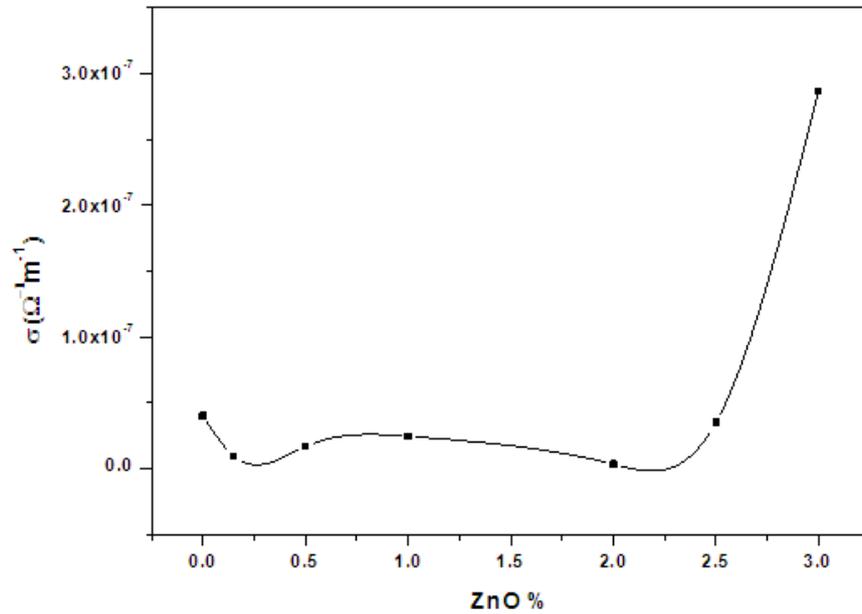
Fig. (8): The obtained values of ac conductivity as a function of ZnO concentrations at 1 kHz and room temperature.

Table (1): Values of the activation energies for pure PVA, ZnO/ PVA nanocomposites, and pure ZnO at different frequencies

f (Hz)	PVA		0.15 %		0.5 %		1 %	
	E_1(eV)	E_2(eV)	E_1(eV)	E_2(eV)	E_1(eV)	E_2(eV)	E_1(eV)	E_2(eV)
1000	0.36	0.99	0.54	0.91	0.44	0.92	0.52	0.89
10000	0.33	0.97	0.41	0.85	0.40	0.90	0.49	0.75
100000	0.25	0.95	0.34	0.76	0.27	0.92	0.46	0.74
1E6	0.14	0.92	0.14	0.81	0.11	0.78	0.24	0.77
3E6	0.09	0.89	0.12	0.74	0.08	0.73	0.18	0.66
5E6	0.07	0.87	0.10	0.72	0.07	0.72	0.15	0.60

f (Hz)	2 %		2.5 %		3 %		ZnO	
	E_1(eV)	E_2(eV)	E_1(eV)	E_2(eV)	E_1(eV)	E_2(eV)	E_1(eV)	E_2(eV)
1000	0.52	0.82	0.46	0.92	0.44	0.68	0.167	0.93
10000	0.45	0.82	0.42	0.90	0.37	0.56	0.172	0.91
100000	0.31	0.88	0.33	0.91	0.21	0.58	0.157	0.86
1E6	0.15	0.76	0.14	0.82	0.05	0.63	0.156	0.85
3E6	0.13	0.63	0.06	0.76	0.03	0.57	0.144	0.83
5E6	0.11	0.61	0.03	0.72	0.02	0.51	0.142	0.81